# One- and two-dimensional quantum transport in thin gold wires

S. Friedrichowski and G. Dumpich
*Experimentelle Tieftemperaturphysik, Gerhard-Mercator-Universität-GH-Duisburg, Lotharstrasse 1, D-47058 Duisburg, Germany*
(Received 23 April 1998)

We report on magnetoresistance (MR) measurements of thin gold wires of various widths, $w$ between 50 nm and 50 $\mu$m prepared by electron-beam lithography. The MR is measured at temperatures between $T=1.5$ and 25 K using a $^4$He-bath cryostat where magnetic fields up to $B=5$ T can be applied perpendicular to the film plane. Varying the widths of the gold wires we find the ''strength'' of the MR being proportional to $w^{-1}$ consistent with one-dimensional (1D) behavior and constant for wires of larger widths indicating 2D behavior. This allows analyzing the MR data of the various gold wires using detailed theoretical calculations concerning 1D and 2D quantum transport. We obtain the phase coherence length and its temperature dependence, which is almost independent of whether the gold wires show 1D or 2D quantum transport behavior. This additionally confirms the analysis of the MR data and exhibits that the phase coherence length displays intrinsic scattering properties. [S0163-1829(98)06136-0]

## I. INTRODUCTION

The quantum mechanical properties of electrons, i.e., the wave character of electrons modifies their transport behavior by weak electron localization (WEL) and enhanced electron-electron-interaction (EEI) effects.[1] These effects, which are well known and well understood precisely allow us to describe quantum transport of electrons in one, two, and three dimensions (1D,2D,3D) by theoretical calculations.[2,3] However, from the experimental point of view it is rather difficult to accurately define conditions where thin metallic films or wires behave 1D- or 2D-like with respect to quantum transport. One expects that 1D or 2D behavior occurs if the width $w$ of thin wires or the thickness $t$ of thin films are much less than the phase coherence length $L_\phi$, which is the relevant length scale for the interference of electron waves.[4] However, since $L_\phi$ strongly depends on temperature as well as on disorder (typically $L_\phi$ decreases with increasing temperature and disorder), the phase coherence length $L_\phi$ can become of the order of the thickness $t$ of the films or the width $w$ of wires ($L_\phi \approx t$, $L_\phi \approx w$). In these cases it is rather difficult to define precisely the dimensionality of the samples with respect to quantum transport.

For thin gold films that are highly inhomogeneous (i.e., with large voids and open channels) we have shown that the presence of 2D quantum transport can additionally be controlled by measuring the MR applying magnetic fields perpendicular as well as parallel to the film plane, since for 2D films the MR is strongly anisotropic, but for 3D samples it is isotropic.[5]

In this paper we report on the temperature and magnetic-field dependence of the resistance for thin gold wires of various width $w$ prepared by electron-beam lithography (EBL) onto GaAs. We find that 1D quantum transport can clearly be separated from 2D phenomena by systematically varying the width $w$ of thin gold wires. This precisely allows to analyse the MR data using theoretical calculations for 1D and 2D quantum transport. From the analysis we find the phase coherence length $L_\phi$ being almost independent of the width $w$ of the wires, i.e., independent of whether 1D or 2D quantum transport occurs.

## II. EXPERIMENT

Thin gold wires of various width $w$ are prepared by EBL onto GaAs substrates at room temperature. For EBL we use a scanning transmission electron microscope (STEM) with an external interface board. The position of the electron beam is computer controlled using a home-designed software. For the lithography process a thin polymethylmethacylat (PMMA) layer ($t=200$ nm) is spun off onto a GaAs substrate that can be mounted into the specimen holder of the STEM. The desired layout is written by a digitized vector-scan technique without using beam blanking. The typical layout consists of the actual nanostructures (wires, networks, dots, etc.) as well as the contact pads for measuring the electrical resistance. Both structures are produced in one run, but at different magnification ranges. The area of the actual structure is about $40\times40$ $\mu$m, whereas the areas of the contact pads are about $2\times2$ mm. After exposing the PMMA it is developed in a mixture of isopropanol (ISO) and methylisobutylketon (MIBK). The resulting structure (mask) can be controlled by an atomic-force microscope (AFM). After depositing a thin gold layer (typical thickness $t\sim25$ nm) onto the mask, the resist is removed by rinsing the sample in acetone.

For the resistance measurements we use a dc-four-terminal technique where typical currents of $I=1$ $\mu$A are applied. The sensitivity of our setup allows us to determine the resistance with a resolution of $\Delta R/R\approx1\times10^{-5}$. The temperature can be varied between 1.5 and 300 K using a $^4$He-bath cryostat, where magnetic fields up to 5 T can be applied perpendicular to the film plane.

## III. RESULTS

Figure 1 shows a secondary electron micrograph (SEM) of five gold wires used for our resistance measurements and the (four) contact pads prepared by EBL onto GaAs (dark areas). Leads glued onto the gold pads (not shown) connect the wires to the current source and the voltmeter. As one can see from Fig. 1 the wires have a length of $L=32$ $\mu$m and a width of $w=46$ nm. The thickness of the gold wires and the pads are $t=25$ nm as determined by a calibrated (Tolansky)

 

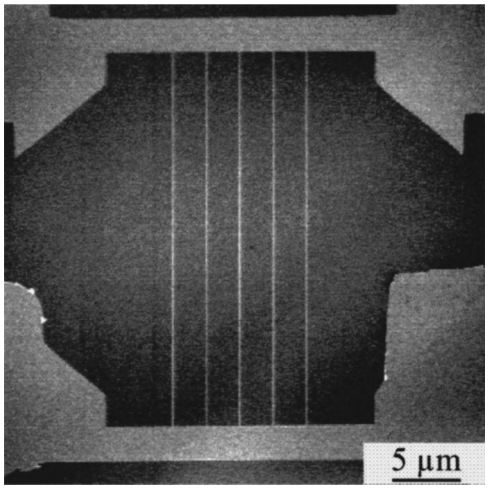


FIG. 1. SEM micrograph of a nanostructured gold film prepared by electron-beam lithography onto a GaAs subtrate. Five wires with a width of $w=46$ nm are connected in parallel to four broad contacts for measuring the electrical resistance. The length of the wires is 32 $\mu$m.

quartz microbalance. To check the ''quality'' of the gold wires we investigated the wires by SEM at higher magnifications (as used for the micrograph in Fig. 1) and moreover by TEM, since we are able to prepare the gold wires onto thin carbon layers. We find the gold wires being continuous without cracks or voids for a typical thickness $t=25$ nm as used for the present structures. The wires are polycrystalline with typical crystal diameters of $\Phi_k=10$ nm.

From the geometry and the total resistance $R$ of the wires we determine the resistivities $\rho$ that are of the order of $\rho \approx 10\ \mu\Omega$ cm at room temperature. Using Drude's law we find—with the Fermi velocity $v_F(\mathrm{Au})=1.39\times10^6$ m/s and the electron density $n(\mathrm{Au})=5.9\times10^{28}$ m$^{-3}$—the electron mean free path being about $l_e\sim10$ nm, which is consistent with our structural information ($l_e\approx\Phi_k$). To compare the resistance data among the various gold wires we define the resistance per square by $R_\square=R(w/l)$, which typically varies between $2\ \Omega/\square<R_\square<12\ \Omega/\square$ for the present gold wires.

Figure 2(a) shows the resistance per square $R_\square$ versus temperature $T$ on the logarithmic scale for a gold wire with $t=20$ nm and $w=51$ $\mu$m (Au1). The dots indicate the experimental data for various magnetic fields $B$ applied perpendicular to the film plane. As one can see from Fig. 2(a) the resistance $R_\square$ increases below $T=5$ K with decreasing temperature exhibiting $R_\square\sim\ln T$-behavior. Applying a magnetic field the resistance $R_\square$ increases (positive magnetoresistance) for all temperatures $T<12$ K, whereas the slopes of the $R_\square(\ln T)$ curves become for $B\geqslant0.05$ T constant as indicated by the straight lines in Fig. 2(a). The value of the slope as given by $\Delta G=[R_\square(1\ \mathrm{K})-R_\square(10\ \mathrm{K})]/R_\square^2(10\ \mathrm{K})$ is $\Delta G=1.64\times10^{-5}(\square/\Omega)$, which has the typical order of magnitude for 2D quantum corrections.[6,7] The inset shows the ''slope'' $\Delta G$ as a function of the applied magnetic field indicating that $\Delta G$ saturates for $B>0{,}1$ T.

Figure 2(b) shows the resistance per square $R_\square$ of a thin gold wire with $t=25$ nm and $w=46$ nm (Au2) versus $T$ on the logarithmic scale for various magnetic fields applied perpendicular to the film plane. As one can see from Fig. 2(b) the resistance $R_\square$ decreases for $B<0.05$ T logarithmically with decreasing temperature. Applying magnetic fields of $B>0.05$ T the resistance logarithmically increases with decreasing temperature. Above $B=0.2$ T the ''slope'' $\Delta G$ saturates as shown in the inset. Figures 3(a) and 3(b) show the magnetoresistance data as defined by $\delta G(B)=[R_\square(B)-R_\square(0)]/R_\square^2(0)$ versus $B$ on the logarithmic scale of the gold wire Au1 and the wire Au2, for various temperatures between $1.5\leqslant T\leqslant25$ K. As one can see the MR is positive for both wires, but there are two remarkable features that are rather different among the two gold wires. For the gold wire with the large width $w=51$ $\mu$m the maximum value of $\delta G$ at the lowest temperature ($T=1.5$ K) is of the order of $\delta G^{\max}\approx40\times10^{-6}\ \Omega^{-1}$, whereas for the small gold wire ($w=42$ nm) it is about $\delta G^{\max}\approx1000\times10^{-6}\ \Omega^{-1}$, which is 25 times larger. Second, whereas $\delta G(B)$ exhibits for the ''wide'' gold wire (Au1) a pronounced maximum at $B\approx1$ T, it shows for the small gold wire (Au2) above $B\approx0.5$ T an almost field independent (saturation) behavior for all temperatures. Please note the different scales of $\delta G(B)$ in Figs. 3(a) and 3(b).

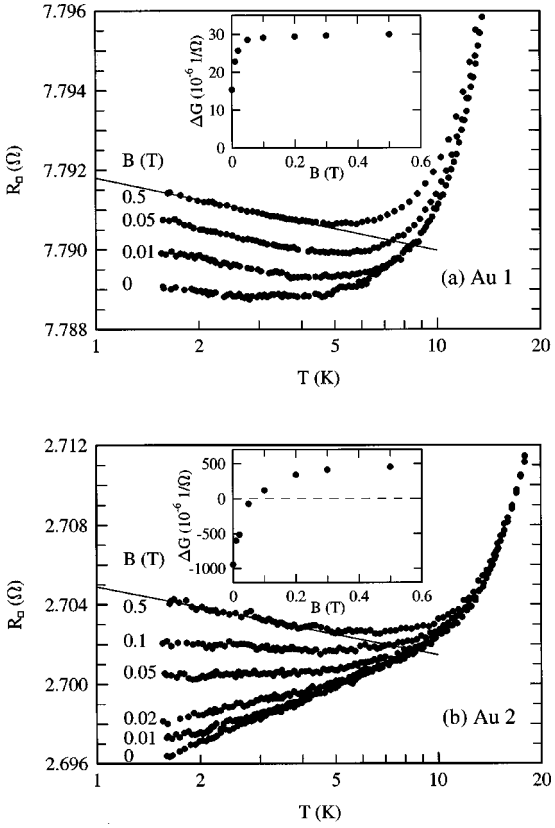


FIG. 2. Resistance per square $R_\square$ vs temperature $T$ within the range $1.5<T<20$ K in the presence of magnetic fields of $B\leqslant0.5$ T perpendicular to the film plane for two different samples (a) Au1 with width $w=50.8$ $\mu$m and (b) Au2 with width $w=46$ nm.

## IV. DISCUSSION

It is rather likely that the different features of the MR behavior are due to the occurrence of 1D or 2D quantum

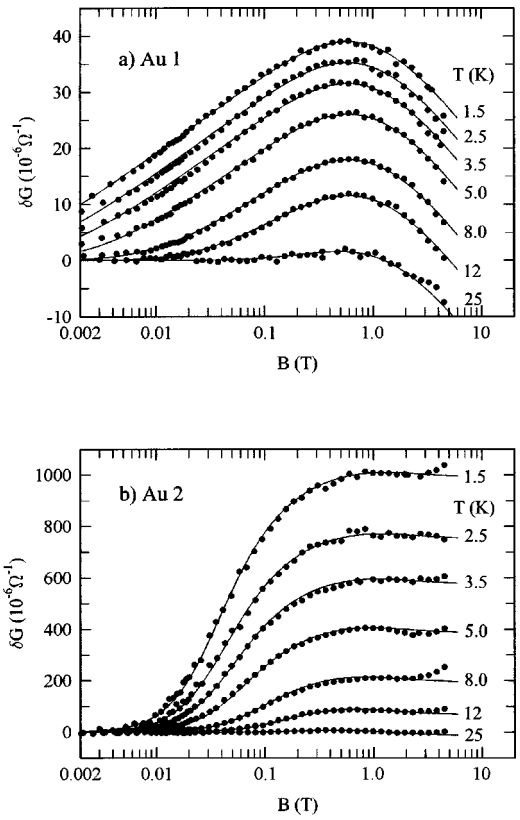


FIG. 3. Magnetoresistance for two nanostructured gold films (a) Au1 and (b) Au2 at various temperatures in the range $1.5 \leqslant T \leqslant 25$ K. Full lines are best fits according to the theory (a) given by Eq. (1) for 2D systems and (b) given by Eq. (2) for 1D systems. Please note the different scales for $\delta G$ in both plots.

transport phenomena, depending on the width of the wires. To check for which width 1D or 2D transport is expected to occur we fabricated a series of gold wires of various widths $w$ and measured the magnetoresistance. Figure 4 shows the ''strength'' of the magnetoresistance $\delta G^{\max}$, which is given by the maximum value of $\delta G(B)$ at a given temperature $T$ plotted versus the width $w$ of the gold wires. The filled circles represent the data for various wires at $T=1.5$ K, the open circles at $T=10$ K, and the filled squares at $T=20$ K. As one can see from Fig. 4 we find at $T=1.5$ K for wires with widths below $w=1$ $\mu$m $\delta G^{\max} \sim w^{-1}$ and above $w=1$ $\mu$m $\delta G^{\max}=$const. At higher temperatures the same behavior occurs, however, the ''cross-over'' from $\delta G^{\max} \sim w^{-1}$ to $\delta G^{\max}=$const shifts to lower widths. This behavior can easily be explained within the framework of 1D and 2D quantum transport. For 1D transport the conductivity is (by definition) given by $\delta\sigma^{d=1} \equiv \delta G w$. In the case of 2D transport one finds $\delta\sigma^{d=2} \equiv \delta G$, where $\delta G \equiv [R_{\square}(B) - R_{\square}(0)]/R_{\square}^2(0)$ is determined from the experimental data $R_{\square}(B)$. From this it follows that $\delta G^{\max} \sim w^{-1}$ and $\delta G^{\max}=$const for wires with 1D and 2D transport properties, respectively. We thus find from our experimental data (Fig. 4) that, e.g., at $T=1.6$ K gold wires with widths $w<1$ $\mu$m behave 1D like, whereas wires with $w \geqslant 1$ $\mu$m are two dimensional with respect to quantum transport. This shows that a distinction between 1D and 2D quantum transport can simply be obtained by analyzing $\delta G^{\max}$ as a function of the width $w$ of thin gold wires. Figure 4 additionally shows that as going to higher

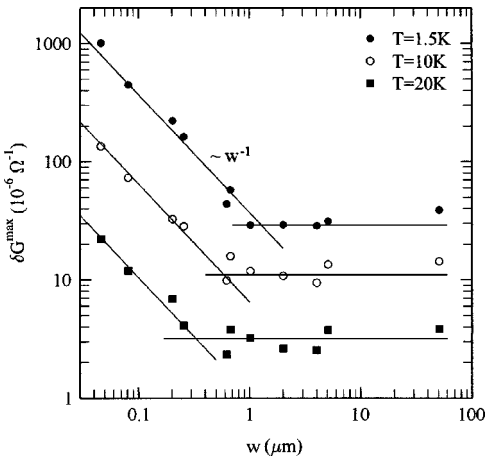


FIG. 4. Maximum value of the magnetoresistance $\delta G^{\max}$ vs the width $w$ for various gold wires at three different temperatures $T=1.5$, 10, and 20 K. Full lines represent the theoretically expected behavior for 1D and 2D systems.

temperatures the range for which the wires behave 1D like becomes smaller. Our further analysis shows that this is due to the fact that the phase coherence length $L_\phi$ becomes smaller for higher temperatures.

According to Fig. 4 we find that the gold wire Au1 with a width of $w=51$ $\mu$m behaves 2D like with respect to quantum transport.[7] We thus analyze the magnetoresistance data of Fig. 3(a) using theoretical expressions for the MR in 2D as given by Hikami, Larkin, and Nagoka:[8]

$$\delta G(B_\perp) = \frac{e^2}{2\pi^2\hbar}\left[f\left(\frac{B_1}{B}\right) - \frac{3}{2}f\left(\frac{B_2}{B}\right) + \frac{1}{2}f\left(\frac{B_\phi}{B}\right)\right] \quad (1)$$

with $B_1 = B_e + B_{so} + B_s$, $B_2 = B_i + 4/3B_{so} + 2/3B_s$, $B_\phi = B_i + 2B_s$ and $f(x) = \Psi(x+1/2) - \ln(x)$ with $\Psi(x)$ the digamma function. The characteristic magnetic fields $B_j$ are correlated via $L_j^2 = \hbar/4eB_j$ to characteristic diffusion length $L_j$ where the suffixes $e$, $i$, so, and $s$ correspond to elastic, inelastic, spin-orbit, and magnetic scattering processes. Using Eq. (1) and choosing appropriate parameters $B_j$ we are able to describe our experimental MR data in Fig. 3(a) in a perfect manner. This is shown by the straight lines in Fig. 3(a) which represent $\delta G(B)$ as given by Eq. (1) for various temperatures between $T=1.5$ and $T=12$ K. For the fitting process we treat the characteristic fields $B_{so}$, $B_s$, and $B_e$ as being temperature independent. Thus, if these fields are fixed for a given temperature (e.g., $T=1.5$ K) and kept constant, there is only one ''free'' parameter, $B_\phi$, which is available to fit $\delta G(B_\perp)$ using Eq. (1) to the experimental MR data in Fig. 3(a) for all temperatures.

For the gold wire Au2 with a width of $w=46$ nm we expect from Fig. 4 to find 1D behavior. We thus analyze our MR data using an expression that is given by Altshuler and Aronov:[9]

$$\delta G(B_\perp) = \frac{e^2}{\pi^2\hbar}\left[\frac{3}{2}\sqrt{\frac{B_w}{B_2}}A(B_2, B_w) - \frac{1}{2}\sqrt{\frac{B_w}{B_\phi}}A(B_\phi, B_w)\right] \quad (2)$$

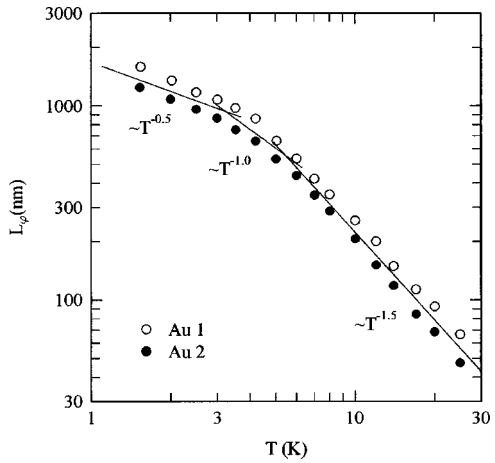


FIG. 5. Log-log presentation of the phase coherence length $L_\phi$ vs temperature resulting from the fits to the MR data in Fig. 3 for the broad wire (Au1) exhibiting 2D behavior and the the small wire (Au2) exhibiting 1D behavior. Full lines represent different power laws for different temperature regions.

with $B_w=\hbar/(4ew^2)$ and $B_2$, $B_\phi$ as defined above and $A(B_j,B_w)=[1+B_2/48B_jB_w]^{-1/2}-1$. Assuming that $B_{so}$, $B_s$ are temperature independent we fit $\delta G(B_\perp)$ as given by Eq. (2) to our experimental data in Fig. 3(b) using suitable parameters $B_j$. The straight lines drawn close to the experimental data show that an excellent description of the MR data within the concept of 1D magnetotransport is possible.

The fitting processes as discussed above allow to determine various characteristic magnetic fields $B_j$ or correspondingly the diffusion length $L_j$. We note that there are no further parameters involved to determine, e.g., the phase coherence length $L_\phi$ from $B_\phi=B_\phi(T)$, since $L_\phi$ is given by $L_\phi^2=\hbar/4eB_\phi$, which contains only universal constants $(\hbar,e)$. Figure 5 shows the phase coherence length $L_\phi$ versus temperature in a double-logarithmic plot for the wide gold wire (Au1) and the small gold wire (Au2). First, it is remarkable to note that the absolute values for $L_\phi$ obtained for the wide (Au1) and for the small (Au2) wire are within a factor of 2 the same. Moreover, even the temperature dependence of $L_\phi(T)$ is equal for both gold wires. This additionally confirms that our analysis of the MR data within the concepts of 1D and 2D quantum transport is correct.

From Fig. 5 we find at high temperatures ($T>5$ K) $L_\phi(T)\sim T^{-1.5}$ and at low temperatures ($T<3$ K) $L_\phi\sim T^{-0.5}$ as indicated by the straight lines. The crossover region might be characterized by a $L_\phi\sim T^{-1.0}$ law. This temperature behavior of $L_\phi(T)$ is typical for thin gold films that are homogenous (with no voids and cracks).[10] As mentioned above, we find the resistivities $\rho_0$ for both gold films—independent on their width $w$—to be almost the same, which involves the fact also that the diffusion constants $D\sim 1/\rho_0$ are quite similar. From this it follows that the phase coherence times $\tau_\phi(T)$ as given by $\tau_\phi=L_\phi^2/D$ are independent on the size of the width of the gold wires. Since magnetic scattering can be neglected in the present temperature region,[11] it follows (with $B_s\ll B_i$) according to Eq. (1) $B_i=B_\phi$ or $L_i(T)=L_\phi(T)$. Thus we directly determine from $L_\phi\sim T^{-0.5}$ and $L_\phi\sim T^{-1.5}$ the temperature dependence of the inelastic scattering times exhibiting $\tau_i\sim T^{-1}$ and $\tau_i\sim T^{-3}$ behavior. This can be well explained by theoretical calculations as resulting from electron-electron and electron-phonon scattering processes, respectively.[12] Moreover, since the observed temperature dependence of the scattering times $\tau_i(T)$ is independent on the width $w$ of the wires; i.e., independent of whether 1D or 2D quantum transport occurs, we conclude that the present scattering data reveal the intrinsic properties of the gold wires.

## V. CONCLUSION

We are able to prepare thin gold wires of various widths between 50 nm and 50 $\mu$m by electron-beam lithography. Magnetoresistance measurements allow precisely to distinguish between 1D and 2D quantum transport at low temperatures by systematically varying the widths of the wires. From the detailed analysis of the MR data we obtain a width-independent phase coherence length and from its temperature dependence the intrinsic electronic scattering properties of thin gold nanowires.

## ACKNOWLEDGMENT

This work was supported by the DFG.

[1] *Localization, Interaction and Transport Phenomena*, edited by B. Kramer, G. Bergmann and Y. Bruynseraede (Springer, Berlin, 1984).

[2] E. Abrahams, P. W. Anderson, D. C. Licciardello, and T. V. Ramakrishnan, Phys. Rev. Lett. **42**, 673 (1979).

[3] G. Bergmann, Phys. Rep. **107**, 1 (1984).

[4] B. L. Al'tshuler, A. G. Aronov, M. E. Gershenson, and Yu. V. Sharvin, Sov. Sci. Rev., Sect. A **9**, 223 (1987).

[5] G. Dumpich, S. Friedrichowski, Z. Phys. B **94**, 3 (1994).

[6] B. L. Al'thuler and A. G. Aronov, in *Electron-Electron Interaction in Disordered Conductors*, edited by A. L. Elfros and M. Pollak (North-Holland, Amsterdam, 1985).

[7] P. A. Lee and T. V. Ramaskrisnam, Rev. Mod. Phys. **57**, 287 (1985).

[8] S. Hikami, A. I. Larkin, and Y. Nagaoka, Prog. Theor. Phys. **63**, 707 (1980).

[9] B. L. Al'tshuler and A. G. Aronov, Zh. Eksp. Teor. Fiz. Pis'ma Red. **33**, 515 (1981) [JETP Lett. **33**, 449 (1981)].

[10] G. Dumpich and A. Carl, Phys. Rev. B **43**, 12074 (1991).

[11] G. Dumpich, S. Friedrichowski, and P. Mikitisin, Thin Solid Films **281**, 368 (1996).

[12] D. E. Prober, in *Localization and Superconductivity*, Vol. 109 of *NATO Advanced Studies Institute Series B: Physics*, edited by A. M. Goldman and S. A. Wolf (Plenum, New York, 1985), p. 231.